THE SWARM ABSOLUTE SCALAR MAGNETOMETER

MAGNETIC CLEANLINESS PROGRAM

F. Alcouffe[1], F. Bertrand[1], T. Jager[1], M. Le Prado[1], J-M. Léger[1], I. Fratter[2]
[1]CEA-Leti, MINATEC Campus, 17 rue des Martyrs, 38054 Grenoble Cedex 9, France, jean-michel.leger@cea.fr
[2]CNES, 18 avenue E. Belin, 31401 Toulouse Cedex 9, France, isabelle.fratter@cnes.fr

ABSTRACT

The Swarm mission selected by the European Space Agency (ESA) as the 3rd Opportunity mission of the Earth Explorer Program will operate a constellation of three satellites dedicated to the most advanced survey of the Earth's magnetic field and its temporal evolution. The magnetic payload aboard each satellite will consist of a Vector Field Magnetometer (VFM) developed by the Danish National Space Center and an Absolute Scalar Magnetometer (ASM) [1] developed by CEA-LETI in partnership with CNES. This instrument shall provide scalar measurements of the magnetic field for the calibration of the fluxgate vector instrument. As a consequence, its accuracy is crucial for the mission's success, and all the parameters affecting it have been consequently thoroughly investigated. This paper focuses on the magnetic cleanliness program that has been implemented throughout the ASM development phases to guarantee its conformity with the performance requirements, from the instrument's design and manufacture to its final qualification tests.

1. INSTRUMENT DESIGN, PARTS SELECTION AND UNITS ASSEMBLY

The ASM instrument consists of an electronic box (Digital Processing Unit) located within the satellite's body and a sensor mounted at the tip of the boom to minimize the magnetic perturbations from the satellite and connected to the electronics box by 9 meter long optical fibers and electrical harnesses (see Figure 1).

Figure 1 Swarm magnetic payload

Given the fact that the magnetic field generated by a magnetic dipole at a distance d decreases with $1/d^3$, potential contributions in terms of magnetic perturbations on the VFM and ASM instruments of the subsystems located within the satellite body are greatly minimized. Consequently, the only specification for the DPUs with respect to magnetic properties consisted in the overall magnetic moment which had to be kept below 25 $mA.m^2$, taking into account both induced and static contributions for a DPU pair (a full cold redundancy has been implemented for the ASM, so that two complete instruments are installed on each satellite). Since this requirement is not very challenging, relatively light selection processes were implemented for the DPU components in that respect and only a few of them were individually characterized due to their very specific magnetic properties. Practically, only two components, both integrated into the laser source, required special attention. The first one was the optical isolator at the output of the fiber laser. This component prevents the injection of backscattered light into the laser cavity and is therefore mandatory to ensure the laser stability. It relies on the Faraday effect (rotation of the laser polarization under the influence of a strong magnetic field, here of the order of 1 T). Although this magnetic field is already quite well confined in such devices, these optical isolators nevertheless exhibited residual magnetic moments of about 20 $mA.m^2$ and had to be further attenuated to comply with the overall magnetic cleanliness requirements. This was achieved thanks to the use of an additional magnetic ring mounted around the isolator to further concentrate its stray fields, thus reducing the perturbation to less than 5% of its original value. The second component which had a significant magnetic signature (although of the order of 20 $mA.m^2$) was an electro optic modulator used in the laser wavelength control loop. A dedicated design analysis revealed that the source of its magnetism was the baseplate on which the components are mounted. To minimize its susceptibility to the thermal environment and ensure stable performances over the [-10 °C / +50 °C] specified temperature range, this baseplate was indeed made of Invar, a material of choice for optical assemblies due to its low thermal expansion coefficient but whose composition (64% Fe, 36 % Ni) unfortunately results in a high magnetic signature. As the electro optic modulator redesign was not compatible with the project planning constraints, this component was dropped and an alternative scheme of laser wavelength modulation based on a direct laser cavity tuning, although less efficient, was finally adopted.

The Figure 2 illustrates the final results obtained for the FM1a DPU (the worst of all manufactured models in that respect) and its corresponding magnetic moment in orbit (modulus of the magnetic moment taking into account both remanent and induced contributions). As can be seen, it is always smaller than 10 $mA.m^2$, thus easily complying with the specifications.

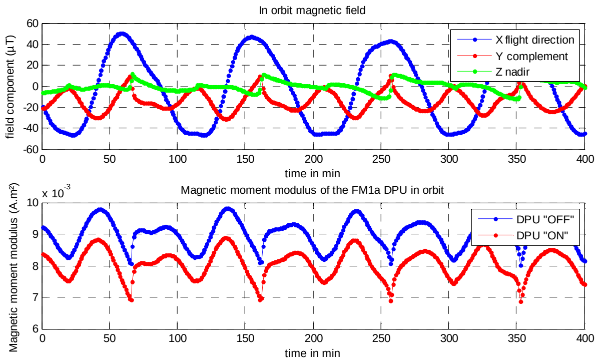

Figure 2 In orbit magnetic moment modulus (FM1a DPU)

Contrary to the DPU, the ASM sensor head clearly requires the most stringent magnetic control, given the very short distances involved between its various components and the helium gas cell where the measurements are carried out. Moreover, since the ASM shall deliver absolute scalar data to calibrate the VFM vector measurements, its accuracy is of utmost importance, since any uncompensated magnetic perturbation will result in systematic errors.

To minimize the structure induced effects, the sensor head is mostly made out of non reinforced PEEK (Polyetheretherketone), a semi-crystalline thermoplastic selected for its very low magnetic susceptibility. In addition, all sensor head subcomponents were individually magnetically screened. This was achieved in a magnetically controlled environment by placing successively each of them directly on the sensor head of a scalar helium magnetometer, while a second reference magnetometer (in this case a LETI NMR instrument) placed a few meters away was operated in parallel. This scheme takes advantage of the very high spatial coherence of the Earth magnetic field over short distances: differential measurements then only depend on the noise of the two magnetometers and are no longer affected by the time fluctuations of the ambient field, which may be several orders of magnitude higher thus usually preventing the detection of small perturbations by a single magnetometer. Thanks to this method, potential contributions as low as 5 pT could be detected.

This procedure led to a drastic parts selection: for instance, more than 50% of the connector pins were rejected, although the best available ‘amagnetic’ grades had been systematically purchased and they all originated from the same production batch.

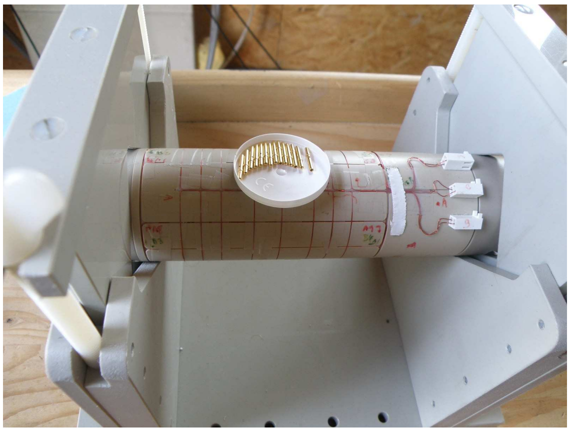

Figure 3 Initial parts screening

It also led to the substitution of several materials used in the Shinsei piezoelectric motor USR 30 S3N (an amagnetic ‘off-the-shelf’ component that drives the sensor head rotor, thus ensuring the magnetometer isotropy), that despite overall excellent characteristics had initially a residual magnetic signature of about 100 pT. The sensor temperature probes were replaced as well, their magnetic properties depending on the actual resistance values due to composition variations.

After the completion of these initial screenings of the sensor head components, which were carried out over a 6 months period, the selected ones were introduced in the sensor assembly dedicated clean room, whose magnetic environment had been previously fully characterized, and the sensor heads were manufactured.

2. HEADING EFFECTS CHARACTERIZATION: ANISOTROPY MEASUREMENTS

As soon as one instrument had been assembled, a characterization of its residual anisotropy (sensor heading errors due to induced effects or remaining remanent contributions) was carried out at the LETI’s Magnetic Tests Facility (Herbeys, France) thanks to a dedicated goniometer.

Figure 4 LMMCF aerial view

To achieve this final check of the magnetometer performances, it was again necessary to resort to a differential scheme since the residual magnetic effects are much too small to be detected otherwise. Typical orders of magnitude of the remaining remanent signature correspond to the influence of a magnetic moment of about 50 pA.m^2 located at 1 cm away from the sensor. This differential scheme makes it possible to reject the ambient field temporal fluctuations with a typical long term baseline stability (this characterization might take up to several hours) of less than 20 pT. The sensor under test is rotated in a homogeneous magnetic field in various configurations:

- a first rotation around the sensor's longitudinal axis oriented along the East-West direction -transverse rotation, quite close to the situation in orbit- allows the detection of any residual remanent effect perpendicular to the sensor axis, as well as induced effects that result from the sensor's slight deviations to the cylindrical symmetry
- a second rotation in a plane containing the ambient magnetic field direction -longitudinal rotation- reveals the remanent effect along the sensor axis and the induced effects resulting from the sensor's cylindrical structure.

Figure 5. Experimental configuration for anisotropy characterization

These two first tests have been processed to establish the perturbation model which will later be used to compensate the residual heading effects. Last but not least, this model has been checked thanks to additional tests (rotation in a horizontal plane for instance, or any configuration different from the ones based on which the model is derived).
Representative results are presented in Figure 6, for a transverse rotation.

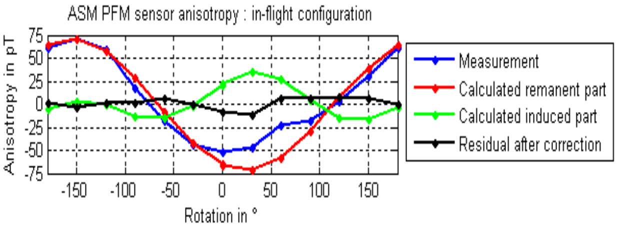

Figure 6. Typical transverse anisotropy

Thanks to that process, the standard deviation of the remaining errors was reduced below 15 pT (1σ) for the seven models manufactured (one Proto Flight Model and six Flight Models), confirming both their excellent workmanship and the effectiveness of the exhaustive magnetic characterizations that were carried out throughout the ASM development process.

The same measurements were repeated after the sensors' integration on the Titanium brackets designed to provide them a mounting interface with the satellite boom, as preliminary tests had shown that their magnetic contributions would significantly degrade the overall ASM performances. While the initial degradation with respect to the sensors stand-alone tests ranged between factors of 3 to 10 for the various flight units, the residual errors after correction were only impacted by less than a factor 2, thus remaining well within the allocated ASM error budget of 0,3 nT. The anisotropy parameters taking into account the bracket contribution were updated in the ASM calibration databases.

3. ACCURATE CHARACTERIZATION OF THE SATELLITE PERTURBATIONS ON THE ASM

Finally, magnetic tests involving again differential scalar measurements were carried out at system level in the magnetic field simulation facility (MFSA) of IABG at Ottobrunn [2] to characterize the perturbations generated by the satellite (induced and remanent effects associated to it, as well as spacecraft electrical currents disturbances with a specific focus on the magneto-torquers and sensors heaters impact) and by the VFM (cross-talk) on the ASM.
Now, since on one hand the deployed satellite can obviously not be rotated in an homogeneous field around the ASM sensor center as it was done for the anisotropy characterization at unit level and on the other hand scalar instruments are only able to detect the projection of the perturbations along the main ambient field direction, this method does not allow to establish a complete magnetic model of the satellite. For instance,

the off-diagonal terms in the matrix representing the induced effects cannot be evaluated by this method, which prevents the direct use of these measurements for the correction of the satellite perturbations onto the VFM. However these tests are the only ones that can be used to verify experimentally with sufficient accuracy the models that are based on vector measurements carried out close to the satellite body to ensure a sufficient signal to noise ratio (differential vector measurements are extremely difficult to obtain since it would imply a pointing accuracy of the order of a few arc seconds, so that practically only field measurements can be exploited). They were therefore conducted as a final ground test during the satellite magnetic qualification.

Figure 7 Differential measurements layout during satellite magnetic tests in IABG's MFSA facility

The dynamic perturbation measurements (electrical disturbances induced by spacecraft currents, in particular magneto-torquers and sensors heaters effects, as well as VFM cross-talk) were characterized thanks to sequences of on-off switches of the corresponding sources for ambient fields set successively along the three main MFSA directions.

Typical VFM cross-talk measurements are shown on Figure 8, which again illustrates the benefit of the selected differential method over simple field measurements (the differential measurements are obtained for sensors positions at respectively 200 cm, 280 cm and 360 cm away from the VFM, while the ASM is only 150 cm away from it and hence is subjected to much higher perturbations).

The signal to noise ratio improvement was under these specific circumstances of the order of 30 dB. The collected data were then compared to the models predictions and confirmed them to a confidence level of less than 20 pT, the error being mostly attributed to residual uncertainties related to the actual position of the reference sensors.

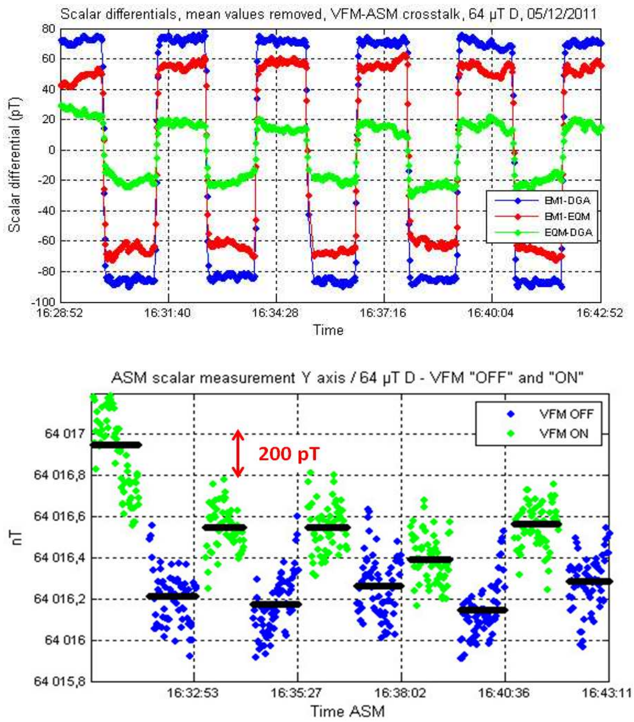

Figure 8 VFM cross-talk measurement (top: differential measurements, bottom: ASM field measurement)

A determination of the satellite remanent and induced effects was also carried out thanks to the same scalar differential measurements method. The reference magnetometers were placed with respect to the satellite main body (with the boom stowed) so as to be representative of the ASM and VFM flight positions once the boom is deployed, and the satellite main body was then moved in and out of the MFSA coils system. By comparing the magnetometers differential readings between these extreme positions, we obtained high accuracy data that are insensitive to the main field fluctuations (due to the high spatial coherence of the applied fields and the temporal stability of the resulting gradients, provided the magnetic environment is not modified during the tests by anthropic perturbations) and therefore only representative of the satellite influence on the magnetometers. Series of measurements were collected for fields of various amplitudes (ranging from +64 µT to –64 µT) along the three main MFSA coils axes, thus making it possible to separate remanent and induced effects. The measurement reproducibility was estimated to be better than 20 pT and preliminary comparisons with the models derived from the facility vector magnetometers show reasonable agreement.

Last but not least, a characterization of the magnetic gradients generated by the MFSA coils for various field settings between the respective positions of the VFM and ASM was conducted. For this ultimate test, the residual errors between the actual scalar gradient measurements and the model predictions were at least ten times lower than the gradients themselves, thus opening the way for an end-to-end VFM calibration on ground.

4. CONCLUSION

Differential scalar measurements have been performed throughout the Absolute Scalar Magnetometer development phases up to the satellite final ground magnetic tests. This allowed first to select the sensors parts in order to minimize their residual magnetic signature and second to evaluate the accuracy of the magnetic data that will be delivered by the ASMs for the three satellites of the Swarm constellation both at instrument and satellite level. This differential method has been adapted to the various rather challenging tests configurations met within the Swarm program. It allowed to demonstrate that the ASM performances meet the mission requirements, with measurement uncertainties below 25 pT. It finally contributed to improve the quality of the magnetic measurements that were carried out at satellite level and check the perturbation models that had been established.

5. REFERENCES

1. J.M. Léger, F. Bertrand, T. Jager, M. Le Prado, I. Fratter and J.C. Lalaurie (2009), SWARM Absolute scalar and vector magnetometer based on Helium 4 optical pumping, In Proceedings of EuroSensors XXIII , Lausanne Switzerland.

2. H.Kuegler, Performance Improvement of the Magnetic Field Simulation Facility MFSA(2004), In Proceedings of the 5th International Symposium on *Environmental Testing for Space Programmes*, ESA SP-558, ESA Publications Division, European Space Agency, Noordwijk, The Netherlands.